University of Kentucky
UKnowledge

Physics and Astronomy Faculty Publications

Physics and Astronomy

2-10-1999

HE I 2.06 Micron Emission from Nebulae

Gary J. Ferland
University of Kentucky, gary@uky.edu

Right click to open a feedback form in a new tab to let us know how this document benefits you.

Follow this and additional works at: https://uknowledge.uky.edu/physastron_facpub

Part of the Astrophysics and Astronomy Commons, and the Physics Commons

HE I 2.06 Micron Emission from Nebulae

He I 2.06 MICRON EMISSION FROM NEBULAE

GARY J. FERLAND

Department of Physics and Astronomy, University of Kentucky, Lexington, KY 40506-0055; gary@pa.uky.edu
Received 1998 August 11; accepted 1998 September 12

ABSTRACT

The spectrum emitted by any astronomical plasma is sensitive to a variety of details, some of which may not be obviously important. This paper describes the sensitivity of the He I 2.06 μm line to the gas opacity at ionizing energies. The intensity of the line relative to a hydrogen line depends on the He$^+$/H$^+$ ratio, but also on the ratio of continuous to He I Lyα line opacity, since this determines whether the Lyα line can scatter often enough to be converted to the 2.06 μm line. The intensity of the infrared line relative to Hβ can change by factors of several depending on details of the radiative transfer of He I Lyα, the gas microturbulence, the dust-to-gas ratio, and the level of ionization.

Subject headings: H II regions — ISM: abundances — line: formation — plasmas — radiation mechanisms: thermal — radiative transfer

1. INTRODUCTION

Large-scale numerical simulations are an interpretive aid in the analysis of spectroscopic observations (Osterbrock 1989). These rely on the complete and accurate inclusion of a host of microphysical processes, and the results can be unexpectedly sensitive to these. Identifying which predictions are sensitive to particular processes is an important part of unraveling the messages in the spectrum.

Ferland et al. (1998) describe recent improvements to CLOUDY, a large-scale plasma simulation code that is used to predict emission spectra of a variety of objects. They were mainly concerned with changes in version C90 and discuss several ways in which its predictions differed from the previous publicly available version, C84.12a. Most large changes in the predicted spectrum were due to the massive improvements in the underlying atomic database that were the result of the Opacity Project and its extensions.

After that paper had been accepted, Blum & Damineli (1999) noticed that the He I 2.06 μm line predicted by C90 differed by about a factor of 2 from those published by Shields (1993), who used C84. This was surprising, since the predicted hydrogen and helium spectra are in excellent agreement. This note discusses the causes for this change, what has been done to improve the physical treatment of the line-forming process in C90.05, and the implications for observations.

2. He I 2.06 μm EMISSION

Figure 1 shows the predicted He I 2.06 μm/Hβ intensity ratios for a series of especially simple model H II regions and several versions of CLOUDY. The nebulae are illuminated by a series of blackbodies with temperatures indicated along the bottom. The cloud is plane parallel, the constant hydrogen density is 10^2 cm^{-3}, and the ionization parameter (the ratio of densities of ionizing photons to hydrogen nuclei) is $10^{-1.5}$. All have gas-phase and grain abundances close to those of the ISM and assume a constant electron temperature of 7500 K. Radial integrations stop at the hydrogen ionization front. The constant-temperature assumption is to ensure that all results will be nearly identical. The predicted hydrogen and helium spectra are in excel-

lent agreement, except for the 2.06 μm line, which does differ by distressing amounts.

Ferland (1980) and Shields (1993) provide summaries of the processes affecting He I 2.06 μm emission at low densities, and Osterbrock (1989, 105) gives a Grotrian diagram. At low densities the population of the upper level is set by the balance between gains due to recombination and losses due to line emission, either as He I Lyα (which then scatters until it escapes or is absorbed) or as the He I 2.06 μm line followed by two-photon emission. The intensity of the IR line relative to a hydrogen recombination line is most strongly affected by the He$^+$/H$^+$ ionic abundance ratio. The initial rise in the line ratio in Figure 1 is due to increasing He$^+$/H$^+$ as the stellar temperature increases.

The intensity of the He I line is also affected by the branching ratio from 2 ^1P,

$$ r = \frac{A_{2p-2s}}{A_{2p-2s} + A_{2p-1s}(P_{\rm esc} - P_{\rm dest})} , \qquad (1) $$

where $P_{\rm esc}$ and $P_{\rm dest}$ are the escape and destruction probabilities, respectively (Rees, Netzer, & Ferland 1989, hereafter RNF; Elitzur 1992). CLOUDY predicts helium emission by solving level populations with moderate-sized atoms including all physical processes. RNF and Ferland et al. (1998) give references for the various escape and destruction probabilities and other techniques used by the code. The escape and destruction probabilities rely on other numerical results (Hummer 1968, hereafter H68; Hummer & Kunasz 1980, hereafter HK80; and Bonilha et al. 1979).

Resonance lines such as He I Lyα have large optical depths, and destruction by background opacity before escape can be a major energy loss. This is especially true when grains are important. He I Lyα has optical depths $\sim 10^4$–10^5 across the He$^+$ zone, so loss due to absorption by the background continuum is large. The destruction probability $P_{\rm dest}$ is related to the dimensionless ratio of continuous to line opacity β, given by (H68)
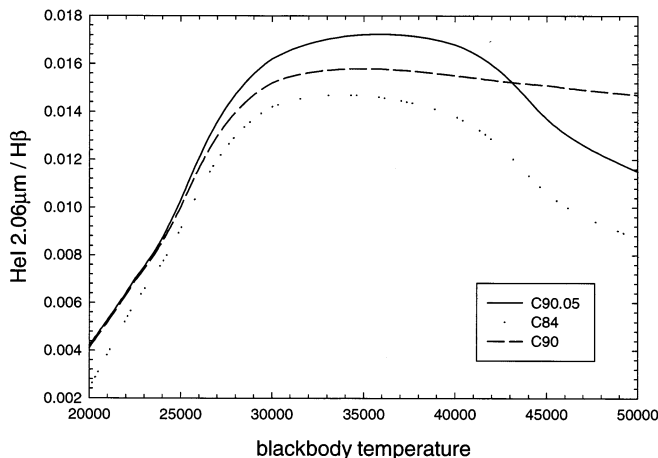
$$ \beta = \frac{\kappa_e}{\kappa_l} . \qquad (2) $$

FIG. 1.—Predicted He I 2.06 μm/Hβ intensity ratios for a series of simple H II regions. Predictions from several assumed efficiencies for destruction by background opacities are shown. The curves marked C84 and C90 are for previous versions of the code, and the predictions using H68 are shown as C90.05. For low stellar temperatures the ratio increases as the He$^+$/H$^+$ ionization increases. It decreases at high temperatures as the He^0/He ratio decreases and destruction of He I Lyα by background opacities becomes more important.

The decrease in the line ratio at high stellar temperature in Figure 1 is due to the He I Lyα line opacity growing so small that destruction by background opacities is especially important.

In general, the destruction probability P_{dest} will be $\beta F(\beta)$ and the problem is to determine the function $F(\beta)$. H68 gives fits to this for the case of complete redistribution in a Doppler core. The destruction probability does not depend on the total line optical depth in this limit. Hummer's results are plotted as the solid line in Figure 2. (The results

have been converted to the line-center optical depths used here; these are a factor of $\pi^{1/2}$ times smaller than the mean optical depths used in the Hummer work.)

HK80 consider incomplete redistribution with damping wings, as would be appropriate for a strong resonance line like He I Lyα. They compute large optical depths but only limited ranges of β. They give the fractions of photons destroyed, and their results can be converted to P_{dest}. Their results also depend on the line optical depth and are plotted as three groups in Figure 2. The figure shows that the H68 and HK80 results agree very well over a wide range in β. This is surprising, since the redistribution functions and analytical methods are very different.

Figure 2 also shows the destruction probability given by equation (15) of RNF as the lower dashed line. This was largely based on Bonilha et al.'s (1979) Monte Carlo results, and was used in version C80 of CLOUDY. RNF noted that this differs by large factors from the Hummer work, but could not identify why (see § 3a of RNF). There is clearly a substantial uncertainty in the escape and destruction probabilities, and this is the ultimate origin of changes in the predicted He I 2.06 μm intensity.

Figure 3 shows the neutral helium fraction and β as a function of depth from the illuminated face of the 50,000 K model shown in Figure 1. This model was chosen because the He I 2.06 μm intensity changed by so much in this case. The He I Lyα optical depth to the point where the He$^+$-He^0 ionization front forms is $\sim 10^5$, although the total He I Lyα optical depth is much larger. Background opacities are very large at the wavelength of the He I Lyα line, owing to grains and hydrogen photoelectric opacity, and the resulting β approaches 10^{-3}. This is well beyond the range in β considered by HK80 for this optical depth. The question is what to do in this limit.

Version C80 of CLOUDY used the RNF expressions. Version C84 used general fits to the HK80 results, and *extrapolated* for large β. In version C90 the routine was changed to not extrapolate beyond the tabulated range of results, since extrapolation is always dangerous. This is the ultimate reason for the differences in the two results in Figure 1. Many of the differences in the results of the current version of the code and those in RNF are due to the different destruction probabilities shown in Figure 2.
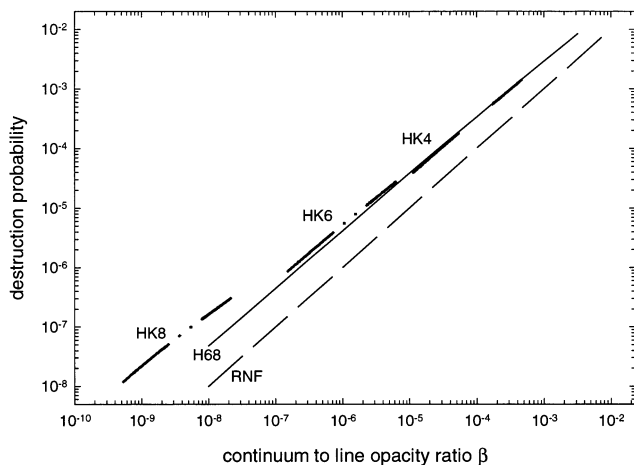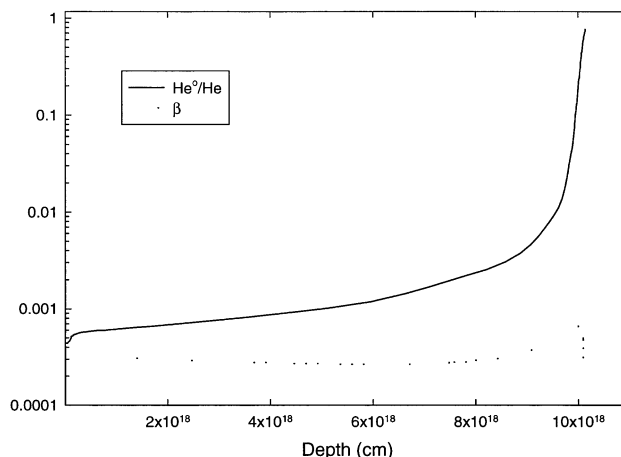

FIG. 2.—Destruction probability predicted by several studies is shown. The solid line is for complete redistribution and a Doppler-only core (H68). The long-dashed lower line is the expression from RNF, based on Bonilha et al. (1979), and was used by CLOUDY through version C80. The three other segments are for different line optical depths from HK80. The curves are for their uniform creation case and total mean line optical depths of 10^4 (HK4), 10^6 (HK6), and 10^8 (HK8). For dusty H II regions, β is larger than any value considered by HK80. Version C84 used HK80 and extrapolated where necessary. Versions C90.00 through C90.04 used HK80 but did not extrapolate. For strongly absorbed lines such as He I Lyα, the H68 results are now used since they apply for any β.

FIG. 3.—Ionization fraction He^0/He (*solid line*) and the ratio of continuum to line opacity β (*dotted line*), as a function of depth for the 50,000 K model from Fig. 1. β is very large, typically $10^{-3.5}$ to 10^{-3}.

Figure 2 suggests that the best approach is to use the expressions from H68 for He I Lyα, and this has been adopted in version C90.05. These have the advantage of extending to all β, and they reproduce the more limited HK80 results for values of β large enough for its effects to be significant. The solid line in Figure 1 shows the predictions resulting from this assumption. The discrepancies between these and the expressions in RNF remain a concern, and an obvious future project.

3. DEPENDENCE ON THE VELOCITY FIELD AND DUST-TO-GAS RATIO

The discussion above has shown that the He I Lyα destruction efficiency strongly affects the predicted intensity of the He I 2.06 μm line. The fact that the results are so sensitive to the continuum-to-line opacity ratio suggests other dependencies. The intensity of the line should be sensitive to the microturbulent velocity field because the line opacity is proportional to the ratio of the oscillator strength to the line width and so decreases with increasing turbulence. It will also depend on the dust-to-gas ratio, since grains are an important continuous opacity source when they are present.

Figure 4 shows the 2.06 μm/Hβ ratio for the 50,000 K model and H68 destruction function, with various values of the microturbulent velocity field. For simulations with no microturbulence, the widths of the helium lines are a few km s^{-1} for nebular temperatures. Turbulent velocities only a bit larger than this begin to make significant changes in the predicted ratio. Similar tests were computed in which the dust-to-gas ratio was varied by factors of 3 above and below the ISM value. The 2.06 μm/Hβ ratio changed by roughly a
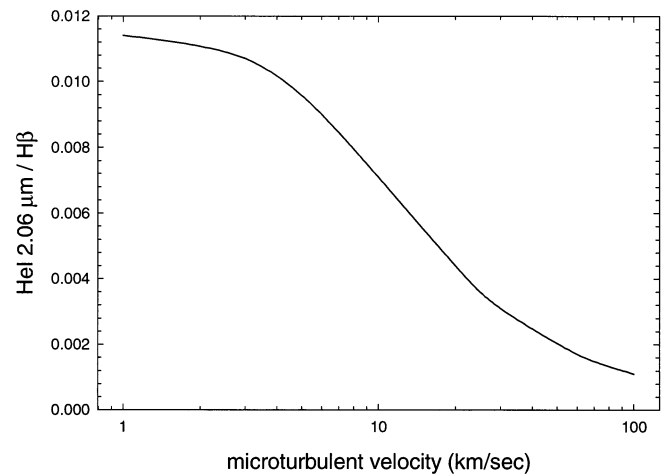

FIG. 4.—He I 2.06 μm/Hβ ratio as a function of microturbulent velocity. The 50,000 K blackbody continuum was used, with all other parameters held fixed.

factor of 2 for these models. These sensitivities could offer a direct and independent probe of the local velocity field and dust-to-gas ratio if the stellar temperature and other parameters could be determined from different observables.

REFERENCES

Blum, R., & Damineli, A. 1999, ApJ, 512, 237
Bonilha, J., French, R., Salpeter, E., Slater, G., & Noerdlinger, P. 1979, ApJ, 233, 649
Elitzur, M. 1992, Astronomical Masers (Dordrecht: Kluwer)
Ferland, G. J. 1980, MNRAS, 188, 669
Ferland, G. J., Korista, K. T., Verner, D. A., Ferguson, J. W., Kingdon, J. B., & Verner E. M. 1998, PASP, 110, 761
Hummer, D. G. 1968, MNRAS, 138, 73 (H68)
Hummer, D. G., & Kunasz, P. B. 1980, ApJ, 236, 609 (HK80)
Osterbrock, D. E. 1989, Astrophysics of Gaseous Nebulae and Active Galactic Nuclei (Mill Valley: University Science Books)
Rees, M. J., Netzer, H., & Ferland, G. J. 1989, ApJ, 347, 640 (RNF)
Shields, J. S. 1993, ApJ, 419, 181